The midblastula transition in *Xenopus* embryos activates multiple pathways to prevent apoptosis in response to DNA damage

Carla V. Finkielstein, Andrea L. Lewellyn, and James L. Maller*

Howard Hughes Medical Institute and Department of Pharmacology, University of Colorado School of Medicine, Denver, CO 80262

Communicated by Joan V. Ruderman, Harvard Medical School, Boston, MA, December 1, 2000 (received for review September 19, 2000)

Apoptosis is controlled by a complex interplay between regulatory proteins. Previous work has shown that *Xenopus* embryos remove damaged cells by apoptosis when irradiated before, but not after, the midblastula transition (MBT). Here we demonstrate that Akt/protein kinase B is activated and mediates an antiapoptotic signal only in embryos irradiated after the MBT. In addition, an increase in xBcl-2/xBax oligomerization and a decrease in xBax homodimerization promote a protective effect against apoptosis only after the MBT. The post-MBT survival mechanism arrests cells in G_1 phase by increasing expression of the cyclin-dependent kinase inhibitor $p27^{Xic1}$. $p27^{Xic1}$ associates with cyclin D/Cdk4 and cyclin A/Cdk2 complexes to cause G_1/S arrest, perhaps allowing more time for DNA repair. Taken together, the results define the DNA damage response as an element of the MBT and indicate that multiple mechanisms prevent apoptosis after the MBT.

Apoptosis is a pathway of cell death required for normal development and differentiation. Evolutionary conservation from nematodes to vertebrates of the general apoptotic death process is evident at the biochemical and cellular levels, albeit with greater complexity in mammals. Vertebrates have evolved entire gene families that resemble single *Caenorhabditis elegans* cell death genes (1, 2), and the products of the mammalian Bcl-2 gene family are functional and structural homologues of CED-9 (3). Their survival function is opposed by two proapoptotic subfamilies, which differ markedly in their relatedness to Bcl-2 (4). The most relevant members of these proapoptotic subfamilies are Bax, which contains BH1, BH2, and BH3 domains and resembles Bcl-2 fairly closely, and Bad, which contains only the central short BH3 domain. Biochemical evidence suggests that for many but not all apoptotic signals, the balance between these competing activities determines the susceptibility to death.

A number of well-characterized cytokines and growth factors promote survival in diverse cell types (5). Signal transduction pathways activated by these factors led to the discovery that the serine/threonine kinase Akt, also known as protein kinase B, is a general mediator of survival signaling through PI3K (6). Akt is activated by phosphorylation at two conserved sites and by direct binding of PI3K lipid products to the pleckstrin homology domain (7).

The cell cycle and apoptosis may be intimately linked because apoptosis regulatory proteins themselves can directly affect the cell cycle machinery (8–11). Cyclin-dependent kinases (cdks) essential for a number of cell cycle transitions are regulated by checkpoints, which can inhibit cell cycle progression in response to ionizing radiation and other DNA-damaging agents (12). A major mechanism of p53-mediated cell cycle arrest proceeds through induction of the cdk inhibitor (CKI) $p21^{CIP1/WAF1}$ (13) that acts on cyclin-cdk complexes to inhibit their kinase activity and block cell cycle progression. Elevated p53 also functions to trigger deletion of damaged cells by apoptosis (14, 15). In *Xenopus* the levels of p53 RNA and protein are high and constant throughout normal oocyte maturation and before and after the midblastula transition (MBT) (16). However, previous results indicate that the maternal apoptotic program in *Xenopus* does not require transcription and is not initiated by increased p53 (17). To date, $p27^{Xic1}$ is the only CKI described in *Xenopus* (18). *In vitro*, $p27^{Xic1}$ preferentially binds to cyclin E/Cdk2 complexes, suggesting that $p27^{Xic1}$ prevents entry into S phase by inhibiting cdks and blocking DNA replication (18).

Before the MBT the cell cycle is rapid and synchronous, oscillating between DNA synthesis and mitosis with no discernible G phases. After the 12th division the cell cycle becomes asynchronous, and G_1 and G_2 phases are present (19, 20). The MBT also marks a dramatic change in the response of the embryo to DNA damage. When ionizing radiation is administered any time before the MBT, *Xenopus* embryos initiate apoptosis after the MBT, and this process is associated with prolonged activation of the cyclin A1/Cdk2 complex (17, 21). However, if ionizing radiation is given after the MBT, embryos are resistant to apoptosis. In this paper we have investigated specific cell cycle molecules and the interaction between pro- and antiapoptotic components in the prevention of apoptosis in embryos irradiated after the MBT. Our results suggest that *Xenopus* embryos prevent apoptosis by multiple mechanisms, including Akt activation, the inactivation of proapoptotic proteins through heterodimerization, and a G_1 arrest mediated by an increase in the level of $p27^{Xic1}$.

Materials and Methods

Preparation of Embryos. Eggs were fertilized *in vitro*, dejellied in 2% cysteine (pH 7.9), and incubated at room temperature as described (17, 18). Embryos were staged according to the method of Nieuwkoop and Faber (22). For time-course experiments, embryos were irradiated at either stage 6 or stage 9, collected at the indicated times, frozen on dry ice, and stored at −80°C. Embryos were homogenized and processed for immunoprecipitation and immunoblotting as described (17, 18). γ-Irradiation (γ-IR) was performed by exposing embryos to 20 Gy (2,000 rads) from a ^{60}Co source as described (17).

Cloning of a *Xenopus* Bax Homolog. An internal *Xenopus* Bax fragment was cloned by PCR amplification of the BH1 and BH2 domains of mouse, rat, and human Bax. The forward primer, 5′-GATGGCAACTTCAACTGGGG-3′, corresponds to the sequence DGNFNWG in the BH1 domain, and the reverse primer, 5′-CAGCCACCCTGGTCTTGGAT-3′, corresponds to the sequence IQDQGGW in the BH2 domain. A *Xenopus* oocyte cDNA library was used as a template in PCR reactions. Samples

Abbreviations: MBT, midblastula transition; cdk, cyclin-dependent kinase; CKI, cdk inhibitor; γ-IR, γ-irradiation, γ-irradiated; GST, glutathione *S*-transferase; xBax, *Xenopus* Bax homolog; WT, wild type; DN, dominant negative; CA, constitutively active.

Data deposition: The sequence reported in this paper has been deposited in the GenBank database (accession no. AF288809).

*To whom reprint requests should be addressed at: Department of Pharmacology, University of Colorado School of Medicine, Box C-236, Denver, CO 80262. E-mail: Jim.Maller@uchsc.edu.

The publication costs of this article were defrayed in part by page charge payment. This article must therefore be hereby marked "*advertisement*" in accordance with 18 U.S.C. §1734 solely to indicate this fact.

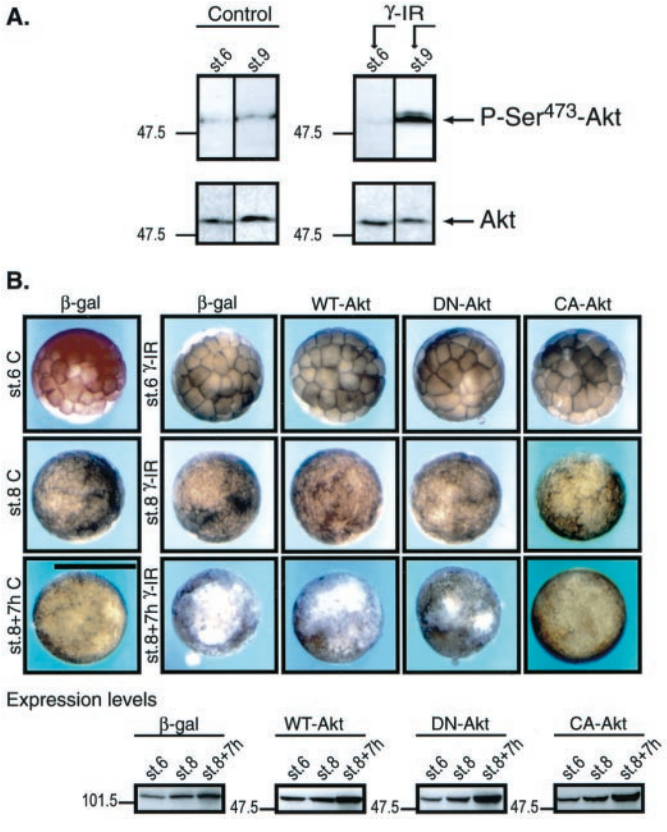

Fig. 1. Phosphorylation of Akt in response to ionizing radiation. (*A*) Embryos were not irradiated (control) or were exposed to γ-IR at either stage 6 or stage 9, collected at different times, and analyzed as described in *Materials and Methods*. The blots were incubated with anti-P-Ser 473 Akt antibody (*Upper*) or anti-Akt antibody (*Lower*) and visualized by enhanced chemiluminescence. The arrows on the right denote the Akt protein and the phosphorylated isoforms. Molecular mass markers (in kDa) are indicated on the left. (*B*) (*Upper*) Embryos were injected at the one-cell stage with β-galactosidase, WT-, DN-, or CA-Akt mRNA and allowed to develop until they reached stage 6 (*Top row*). At that stage, embryos were not irradiated (first column on left) or were treated with ionizing radiation (γ-IR) and allowed to progress through early developmental stages. Embryos were collected and photographed at the time of irradiation (*Top row*, stage 6), at the MBT (*Middle row*, stage 8), and 7 h after the MBT (*Bottom row*), when the morphological changes of apoptosis were conspicuous (scale bar, 1 mm). (*Lower*) At the indicated stages, levels of the indicated expressed proteins were analyzed by Western blotting.

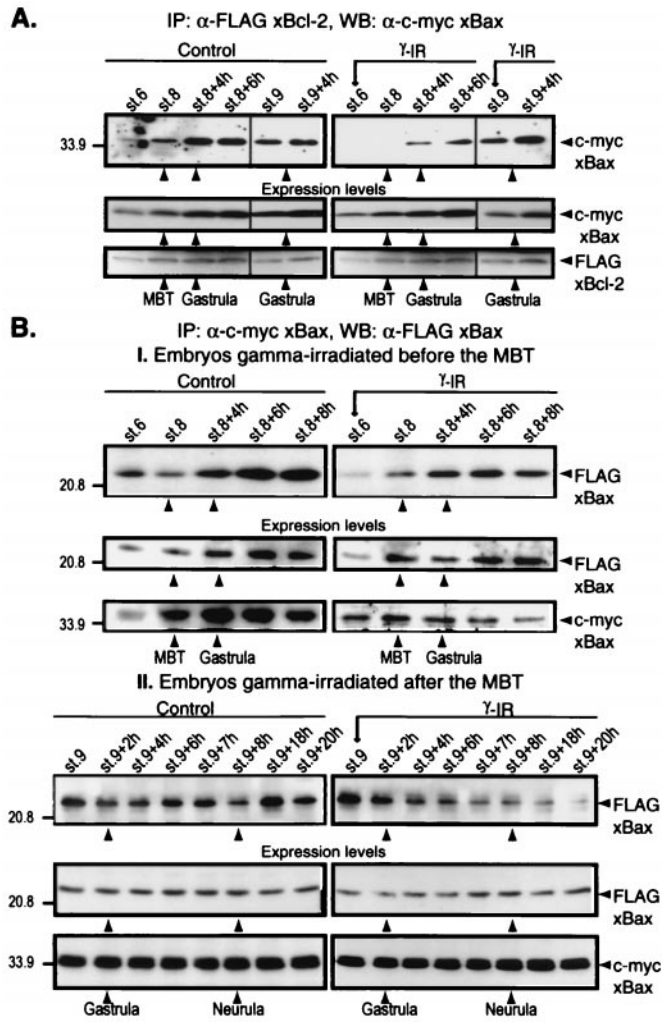

Fig. 2. (*A*) Interaction between xBcl-2 and xBax changes at the MBT. Embryos were injected at the one-cell stage with a mixture of FLAG-tagged xBcl-2 and c-*myc*-tagged xBax mRNAs. The embryos were not irradiated (control) or were irradiated 3 h (stage 6) or 7 h (stage 9) after fertilization, collected at different times, and frozen. Samples equivalent to five embryos were immunoprecipitated with anti-FLAG M2-agarose beads, and the immunocomplexes were subjected to Western blot analysis with anti-c-*myc* antibody. (*B*) Analysis of xBax homodimerization. Embryos were injected at the one-cell stage with FLAG-tagged and c-*myc*-tagged xBax mRNAs, were not irradiated (control) or were irradiated at either stage 6 (*I*) or stage 9 (*II*), and were collected at different times. Samples equivalent to five embryos were immunoprecipitated with anti-c-*myc*-agarose beads, and the immunocomplexes were blotted with anti-FLAG M2 antibody (*I, Top*, and *II, Top*). Total FLAG-xBcl-2, FLAG-xBax, and c-*myc*-xBax expression levels were assessed at all stages by Western blotting with specific anti-tag antibodies (*A* and *B*, *I* and *II*, *Middle* and *Bottom*). Arrows on the right denote the FLAG-tagged or c-*myc*-tagged protein.

were subjected to 35 cycles at 94°C for 1 min, 46°C for 1 min, and 72°C for 2 min. An amplified fragment of 169 bp contained an insert homologous to the BH1-BH2 region in mouse Bax. The cloned fragment was radiolabeled and used to screen a *Xenopus* oocyte cDNA library. The full-length *Xenopus* Bax homolog (xBax) cDNA was cloned into pCS2 + FLAG and pCS2 + (c-*myc*)$_6$ tag vectors (Novagen).

Microinjection. FLAG- or c-*myc*-tagged xBax and/or FLAG-tagged xBcl-2 mRNAs were microinjected into embryos to a final intracellular concentration of 0.42 μM each. Wild-type (WT), dominant negative (DN), and constitutively active (CA) mouse Akt cDNAs (Upstate Biotechnology, Lake Placid, NY) were cloned into pCS2 +. mRNA was synthesized with a mRNA mMESSAGE mMACHINE kit (Ambion, Austin, TX), and 1 ng of each mRNA preparation was microinjected into embryos. Microinjections were performed at the one-cell stage, between 30 and 70 min after fertilization. After microinjection, embryos were exposed to γ-IR and used for time-course experiments.

Antibodies, Immunoblotting, and Immunoprecipitation. Antisera raised against full-length *Xenopus* cyclins A1, A2, B1, and B2; Cdk4; and p27^{Xic1} have been described (17, 18, 23, 24). Akt and phospho-Akt (Ser^{473}) antibodies were obtained from New England Biolabs, anti-FLAG M2 was obtained from Sigma, and anti-c-*myc* 9E10 antibody was produced in the Tissue Culture/Monoclonal Antibody Core Facility at the University of Colorado Cancer Center (National Institutes of Health Grant CA-P01-46934).

Production, Purification, and Assay of Recombinant Cyclin D/Cdk4. *Xenopus* Cdk4 was expressed in baculovirus-infected Sf9 cells as a fusion protein with GST. The *Xenopus* cdk4 gene (a kind gift

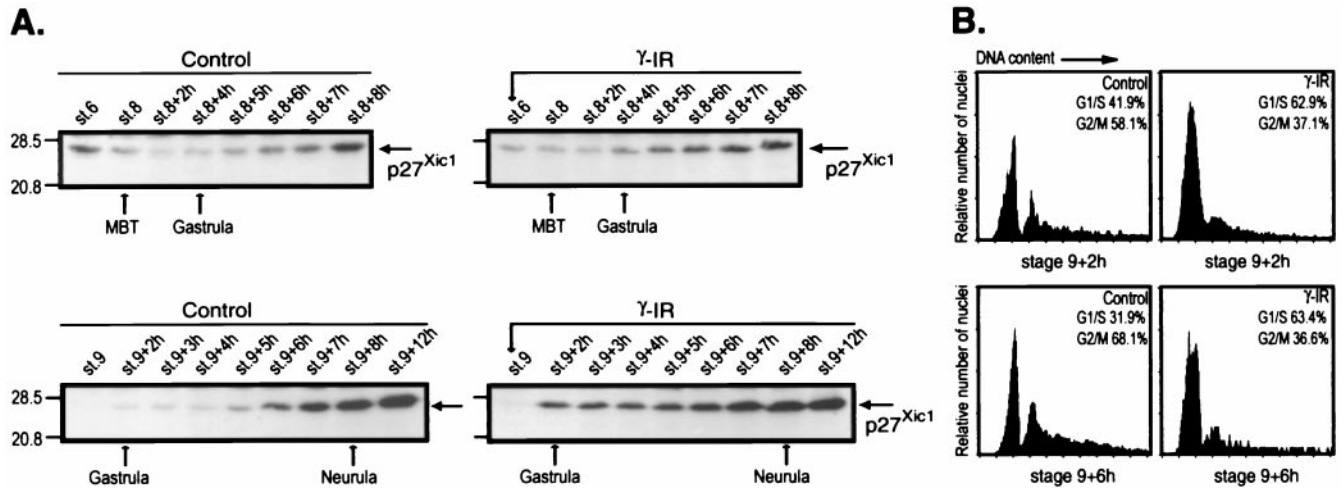

Fig. 3. (*A*) Analysis of the level of p27^{Xic1} in embryos irradiated either pre- or post-MBT. Embryos were not irradiated (control) or were irradiated (γ-IR) at the indicated stages, and samples were collected at the indicated times and analyzed by Western blotting with anti-p27^{Xic1} antibody. One embryo equivalent was loaded per lane. (*B*) Cell cycle profile of irradiated embryos. Embryos were irradiated at stage 9 and collected 2 and 6 h after irradiation. Embryonic nuclei were prepared from a single sibling group and analyzed by flow cytometry as described in *Materials and Methods*. Stages of the cell cycle are defined by DNA content, as measured by fluorescence intensity.

of Dr. T. Hunt, Imperial Cancer Research Fund, South Mimms, U.K.) was cloned into the baculovirus expression vector pVL1392 (Invitrogen, San Diego, CA), modified to encode a GST tag. Sf9 cells were coinfected with baculoviruses expressing *Xenopus* cyclin D1 and GST-Cdk4 and the complex was purified as described (18). The purified cyclin D/Cdk4 and cyclin A2/Cdk2 complexes were diluted in kinase buffer [50 mM Hepes (pH 7.5)/10 mM $MgCl_2$/1 mM DTT/2.5 mM EGTA/10 mM β-glycerophosphate] and preincubated with the indicated amounts of GST- p27^{Xic1} or GST alone (control) at 23°C for 30 min. For cyclin D/Cdk4, each sample was added to an equal volume containing 0.2 mg/ml of the C-terminal half of human retinoblastoma protein. Samples were incubated at 30°C for 20 min, and the reaction was terminated by the addition of 5× SDS-PAGE sample buffer. Samples were electrophoresed on gels and analyzed by Western blotting with a phosphospecifc antibody to Ser ^{795} in human retinoblastoma protein (New England Biolabs). The bands were quantified by densitometric analysis with an AlphaImager 2000 system. The activity of the cyclin A2/Cdk2 complex was measured as described with histone H1 as a substrate (24).

Fluorescence-Activated Cell Sorter Analysis. Embryos were incubated at room temperature, collected at the indicated stages, and washed three times in a 55-mm culture dish as described (26). One hundred embryos were homogenized in 400 μl of buffer containing 0.25 M sucrose by repeated pipetting with a micropipetter. Additional buffer containing 0.25 M sucrose was added to a final volume of 1 ml. An additional 4.75 ml of buffer containing 0.05% Nonidet P-40 and 2.2 M sucrose was added and mixed thoroughly by vortexing. The homogenate was layered onto 500 μl of a 2.2 M sucrose cushion in a 13 × 51 mm centrifuge tube and centrifuged at 130,000 × *g* for 2 h at 4°C. After the lipid and yolk supernatant was removed, the black pigment granule and nuclear pellet was resuspended in nuclear buffer (26) and layered over a 170-μl cushion of 80% glycerol in a microcentrifuge tube. After centrifugation at 3,300 × *g* for 10 min at 4°C, the supernatant was removed and the pellet was resuspended in the appropriate volume of nuclear buffer. An equal volume of Krishan's stain was added, and the samples were kept overnight at 4°C. Flow cytometry was performed with a Coulter Epics-XL flow cytometer at the Flow Cytometry Core Facility at the University of Colorado Cancer Center. Percentages of total nuclei present in each phase of the cell cycle were calculated with Coulter SYSTEM II software.

Results

Activation of Akt Inhibits Apoptosis in Embryos Irradiated After the MBT. *Xenopus* uses programmed cell death to remove damaged cells in embryos exposed to ionizing radiation before the MBT; however, when treated with the same dose of γ-IR after the MBT, embryos do not undergo apoptosis (17). At present, nothing is known about the pathways involved in protection from apoptosis after the MBT. We sought to determine whether Akt might provide protection from apoptosis after the MBT. Phosphorylation of either Thr^{308} or Ser^{473} leads to partial activation of Akt *in vitro*, and phosphorylation of both residues results in a synergistic activation of the enzyme (27). To assess the activity of Akt, phosphorylation of Ser^{473} was evaluated with the use of a phosphospecific antibody that reflects *Xenopus* Akt activation (28).

Embryos were irradiated either at stage 6 (pre-MBT) or at stage 9 (post-MBT) and collected at different times after irradiation. Phosphorylation of Ser^{473} increased much earlier and to a higher level in embryos irradiated after the MBT (stage 9) compared with untreated embryos or those irradiated before the MBT (stage 6), with no change in the total level of Akt (Fig. 1*A*). These results suggest that Akt kinase activity may be involved in the antiapoptotic signaling pathway induced by ionizing radiation in embryos irradiated after the MBT. To evaluate this possibility directly, we determined whether constitutively active Akt can prevent apoptosis in embryos irradiated before the MBT. Embryos were injected with mRNA encoding WT, DN, or CA mouse Akt, irradiated at stage 6 (Fig. 1*B, Top row*), and analyzed for the morphological signs of apoptosis. All treated embryos reached the MBT without any evident morphological change (Fig. 1*B, Middle row*). Seven hours after the MBT, embryos expressing β-galactosidase, WT-Akt, or DN-Akt presented an abnormal pigmentation on the animal pole and membrane-bound bodies (apoptotic bodies) (Fig. 1*B, Bottom row*). These features are characteristic of ionizing-radiation-induced apoptosis in early *Xenopus* embryos (17). CA-Akt-injected embryos did not exhibit apoptotic features at this time (Fig. 1*B, Bottom row*). However, even CA-Akt-expressing embryos underwent apoptosis at later times (data not shown), indicating that CA-Akt is able to delay apoptosis but not completely abolish it.

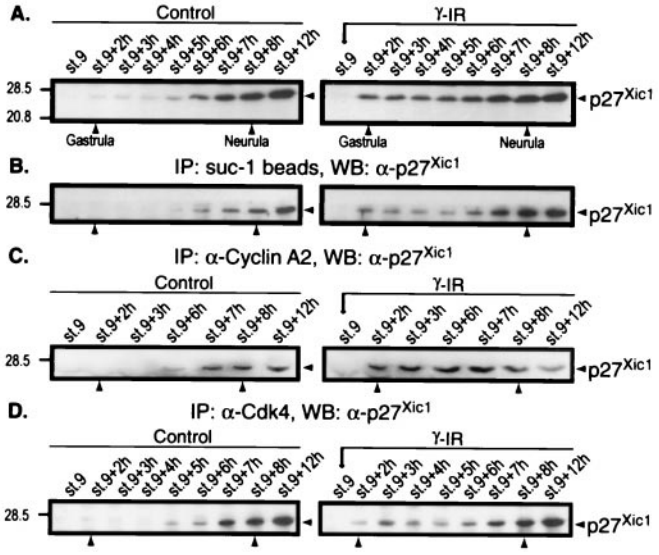

Fig. 4. Targets for p27^{Xic1} *in vivo*. Embryos were not irradiated (control) or were irradiated after the MBT (stage 9 γ-IR), collected at different times, and frozen. (*A*) The total level of p27^{Xic1} at the indicated times. (*B*) Samples equivalent to five embryos were precipitated with p13^{suc-1} beads, and the bound proteins were analyzed by Western blotting with anti-p27^{Xic1} antibody. (*C*) Association of p27^{Xic1} with cyclin A2 complexes was detected by immunoprecipitation with cyclin A2 antibody and analysis of the precipitates by Western blotting with anti-p27^{Xic1} antibody. (*D*) Samples from embryos irradiated after the MBT were immunoprecipitated with anti-Cdk4 antibody and blotted with anti-p27^{Xic1} antibody.

Because there are multiple downstream effectors of Akt in other cell types, it is not yet clear what substrates of Akt prevent apoptosis in the *Xenopus* system.

The xBcl-2/xBax Ratio Controls the Rate of Programmed Cell Death in γ-IR Embryos. One common mechanism for regulating apoptosis is competing dimerization among Bcl-2 family member proteins (4). Bax and Bcl-2 are two of the gene products that can regulate apoptosis through dynamic changes in their interaction (29). Therefore, we assessed whether the association of Bcl-2 with Bax is altered in γ-IR embryos. To explore this possibility, xBax was cloned as described in *Materials and Methods*. The full-length xBax cDNA contains an ORF of 221 amino acids with a predicted molecular mass of 24.2 kDa, and the methionine initiation codon is surrounded by a Kozak (30) consensus sequence. *Xenopus* Bax shares 64% overall identity with the corresponding human and mouse homologs and more than 90% identity in the BH1, BH2, and BH3 domains. The C-terminal region includes the transmembrane domain characteristic of integral membrane proteins. mRNAs encoding the *Xenopus* Bcl-2 and Bax homologs were used in further experiments.

Embryos were injected shortly after fertilization with FLAG-tagged xBcl-2 and c-*myc*-tagged xBax mRNAs, then irradiated at either stage 6 or stage 9, and collected at different times. Control embryos were injected with the same mRNA preparations but not irradiated. xBcl-2/xBax heterodimers were detected by immunoprecipitation of the samples with FLAG-specific antibody and immunoblotting with c-*myc* antibody. The amount of xBcl-2/xBax heterodimers detected in control embryos increased until the MBT and then remained constant (Fig. 2*A, Top*). However, embryos irradiated at stage 6 showed decreased xBcl-2/xBax association compared with controls at the same stages (Fig. 2*A, Top*). In contrast, when embryos were irradiated after the MBT the amount of xBcl-2/xBax heterodimers was increased compared with control (Fig. 2*A, Top*). These results correlate with the phenotype observed

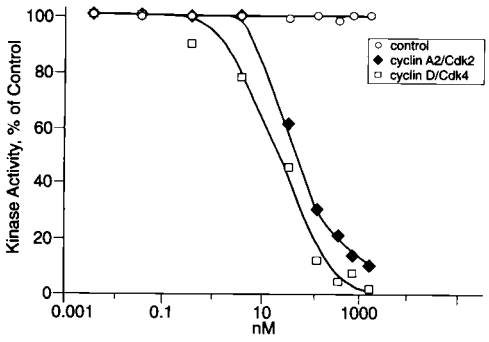

Fig. 5. Inhibition of cyclin D/Cdk4 and cyclin A2/Cdk2 activity by p27^{Xic1}. Purified cyclin D/Cdk4 or cyclin A2/Cdk2 complexes were preincubated with the indicated amounts of GST-p27^{Xic1} or GST alone (control), and the kinase reaction was performed with either the C-terminal half of human retinoblastoma protein (hRb) as substrate for Cdk4 or histone H1 for Cdk2, as described in *Materials and Methods*.

with γ-IR in each case, suggesting that the apoptotic mechanism elicited before the MBT is xBax-dependent and that xBcl-2 antagonizes the apoptotic effect of xBax in a dominant fashion in embryos irradiated after the MBT.

Reduced antiapoptotic interaction between xBax and xBcl-2 could lead to increased homodimerization of Bax, which also favors apoptosis. To test xBax/xBax association, embryos were injected shortly after fertilization with FLAG- and c-*myc*-tagged xBax mRNAs, irradiated at the indicated stages, collected at different times, and analyzed as described in *Materials and Methods*. Embryos irradiated at stage 6 showed a detectable level of xBax homodimers in the stages where no xBcl-2/xBax heterodimer association was observed (see stage 6 and stage 8 in Fig. 2*A, Top*, and Fig. 2*B, I, Top*). Interestingly, in embryos irradiated after the MBT there is a strong correlation between the increased level of heterodimers formed and the decreased level of xBax homodimers detected (*cf.* Sf9 + 4 h in Sf9 and Fig. 2*A, Top*, and Fig. 2*B, II, Top*).

p27^{Xic1} Is Increased and G_1 Arrest Occurs in Embryos Irradiated after the MBT. In mammalian cells the response to DNA-damaging agents includes a delay in progression through the cell cycle (12, 31).

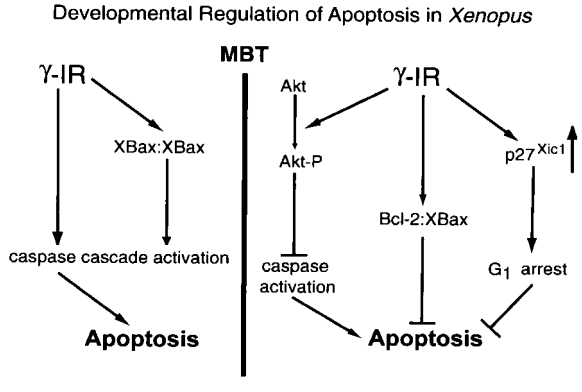

Fig. 6. Model of apoptosis regulation in *Xenopus* embryos. Ionizing radiation promotes apoptosis in embryos irradiated before the MBT by triggering different proapoptotic factors, including the homodimerization of xBax, and caspase cascade activation. Apoptosis is prevented in embryos irradiated after the MBT by the coordinated action of antiapoptotic stimuli. Survival signaling pathways act at at least three levels: by promotion of cell cycle delay by increasing the amount of p27^{Xic1} and its association with the complexes involved in the G_1/S transition, by inactivation of proapoptotic molecules by heterodimerization, and by activation of antiapoptotic pathways like Akt.

Previous work has shown that the cell cycle is lengthened in pre-MBT embryos injected with $p27^{Xic1}$ (32). Therefore, we investigated the possibility that $p27^{Xic1}$ could be involved in the survival response of embryos exposed to γ-IR after the MBT. Embryos were exposed to ionizing radiation at either stage 6 or stage 9, collected at different times, and analyzed for $p27^{Xic1}$ expression. Immunoblotting revealed that developmental changes in $p27^{Xic1}$ were not appreciably different in control embryos versus those that had undergone apoptosis in response to γ-IR before the MBT (Fig. 3*A, Upper*). However, there was a rapid, dramatic increase in the level of $p27^{Xic1}$ in embryos exposed to γ-IR after the MBT compared with controls at the same stages (Fig. 3*A, Lower*). Thus $p27^{Xic1}$ accumulates in response to γ-IR after the MBT and may be involved in the decision to arrest the cell cycle and avoid apoptosis.

To investigate directly the possibility that cell cycle progression is delayed in γ-IR embryos after the MBT, we quantified changes in the cell cycle by fluorescence-activated cell sorting of isolated nuclei. The resulting histograms show that the G_1 peak became increasingly pronounced 2 h after irradiation at stage 9, commensurate with a decrease in the number of G_2/M-phase nuclei compared with control. Six hours after stage 9, γ-IR embryos still exhibited a reduced G_2/M phase compared with controls at the same stage, indicating a prolonged G_1 arrest (Fig. 3*B*).

Increased $p27^{Xic1}$ Binds to Cyclin D/Cdk4 and Cyclin A2/Cdk2 *in Vivo*. We next studied possible targets of $p27^{Xic1}$. CKIs of the Cip/Kip family inhibit cyclin D-, E-, and A-dependent kinases (33). No change in total cyclin B1, B2, E1, Cdc2, Cdk2, or Cdk4 levels was evident in embryos exposed to γ-IR at any stage compared with control (data not shown). To determine the binding partners of $p27^{Xic1}$ in embryos exposed to ionizing radiation after the MBT, samples were collected at different times after irradiation, and analyzed for the presence of $p27^{Xic1}$ by Western blotting. Embryo extracts were incubated with $p13^{Suc1}$ beads, and the bound complexes analyzed for $p27^{Xic1}$. $p27^{Xic1}$ was detected on $p13^{Suc1}$ beads (Fig. 4*B*) at a level reflecting the increased abundance of $p27^{Xic1}$ in the extract from irradiated embryos (Fig. 4*A*). This result suggests that $p27^{Xic1}$ binds to any of the following complexes: cyclin E/Cdk2, cyclin B1/Cdc2, cyclin B2/Cdc2, cyclin A1/Cdk2 and/or cyclin A1/Cdc2, and cyclin A2/Cdk2. However, it is unlikely that $p27^{Xic1}$ binds to the cyclin A1 complexes, because most cyclin A1 has been degraded by the time of $p27^{Xic1}$ appearance (17, 24). Moreover, most cyclin E is degraded between 6 and 7 h after fertilization, coincident with the onset of the MBT (24, 34).

Immunoprecipitation results indicate that cyclin A2/Cdk2 immunocomplexes bind increased $p27^{Xic1}$ beginning shortly after irradiation (Fig. 4*C*), whereas cyclin B/Cdc2 does not bind $p27^{Xic1}$ significantly until 12 h after stage 9, and this difference in binding pattern is unaffected by irradiation (data not shown). $p27^{Xic1}$ also binds Cdk4 (Fig. 4, *D*) in embryos irradiated after the MBT, which might also promote cell cycle arrest in the G_1 phase. Because both Cdk4 and Cdk2 activity are needed for the G_1/S transition (35), the overall results presented here correlate well with Fig. 3*B*, where an increased number of cells is arrested in the G_1 phase of the cell cycle after irradiation.

Because $p27^{Xic1}$ associates *in vivo* with Cdk2 and Cdk4 complexes, we next studied the possibility that this interaction inhibits the kinase activity of the complexes in an *in vitro* assay. Mutational analysis indicates that Ser^{795} in the Rb pocket is the preferred phosphorylation site for cyclin D/Cdk4 (36, 37). Thus, phosphorylation of Ser^{795} was used to determine whether the binding of $p27^{Xic1}$ to Cdk4 led to inhibition of its activity. Purified cyclin D/Cdk4 was preincubated with different concentrations of $p27^{Xic1}$, and the activity was measured as described in *Materials and Methods*. The result, shown in Fig. 5, indicates that $p27^{Xic1}$ is able to completely inhibit the activity of the cyclin D/Cdk4 complex at a concentration of 75 nM; a similar concentration of $p27^{Xic1}$ was able to inhibit the histone H1 kinase activity of cyclin A2/Cdk2 (Fig. 5). Therefore, the association of $p27^{Xic1}$ with both Cdk2 and Cdk4 may delay the G_1/S transition after γ-IR, perhaps allowing more time for DNA repair before triggering of the apoptotic program, which might occur if S phase were initiated with damaged DNA.

Discussion

The findings reported here show that in *Xenopus* embryos the apoptotic pathway induced by ionizing radiation is blocked after the MBT by the coordinated activation of a broad spectrum of negative regulators of apoptosis and cell cycle progression. One negative regulator is the protein kinase Akt, which mediates survival signals in other systems (6). Our data demonstrate that Akt is activated for an antiapoptotic effect only in embryos irradiated after the MBT (Fig. 1). The Akt pathway might act at several different levels. Our results show that the steady-state level of Bcl-2 remains constant after irradiation at any stage (data not shown). Nevertheless, Akt may alter the level of free Bcl-2 by a posttranslational mechanism that influences the competing dimerizations among pro- and antiapoptotic proteins and therefore the susceptibility to cell death (Fig. 2). An alternative route of Akt action may involve the phosphorylation of two major components in the cell death pathway: Bcl-2 family members such as Bad (38), which block apoptosis, and the CED-3/ICE-like protease family, which executes the apoptotic pathway (39). Akt has been implicated in the phosphorylation and inactivation of Bad in several systems that overexpress both Akt and Bad (38, 40). Furthermore, Akt can counteract effects of proapoptotic Bcl-2 family members that lack Akt phosphorylation sites by inhibiting both the release of cytochrome *c* and alterations in mitochondrial membrane potential induced by multiple apoptotic stimuli (41). It is possible that Akt may promote cell survival in *Xenopus* embryos by any of these mechanisms; however, work in this area would require cloning of *Xenopus* Bad, Bik, and Bak homologs.

Human but not mouse caspase-9 can be directly regulated by Akt-mediated phosphorylation (42, 43) at Ser^{183} (RTRTGS) and Ser^{196} (RRRFSS). Both sites are conserved in *Xenopus* caspase-9 (44). The ability of caspase-3 to trigger downstream apoptotic events relies on its activation by caspase-9. Human pro-caspase-9 can be directly regulated by Akt because its autocatalytic self- and *trans*-processing is inhibited by Akt-mediated phosphorylation (45). This mechanism, together with the phosphorylation of Bad, could provide alternative or redundant mechanisms for Akt-mediated cell survival. Our results show Akt activation only in embryos irradiated after the MBT, where no apoptosis was observed (Fig. 1*A*) and no caspase activity was detected (data not shown). Ectopic expression of a constitutively active form of Akt was able to delay apoptosis but not completely abolish it in embryos that normally undergo apoptosis after irradiation (Fig. 1*B*). These results support Akt as an antiapoptotic mediator after γ-IR but suggest that other mediators are also required to completely prevent cell death.

Although neither xBax or xBcl-2 showed any change in abundance as a result of ionizing radiation, there was a change in the proportion of antiapoptotic xBax complexes after the MBT. Our data indicate that xBax oligomerization is favored in embryos irradiated before the MBT (Fig. 2*B*), and prevention of apoptosis after the MBT is correlated with an increased level of antiapoptotic xBcl-2/xBax dimers and a decreased proapoptotic xBax homodimer population (Fig. 2*A*). Inasmuch as overexpression of xBcl-2 or xBax can prevent or promote apoptosis in embryos, respectively (ref. 46 and data not shown), the results suggest that the ratio of xBcl-2 to xBax in dimers governs susceptibility to cell death, presumably by regulating the release of cytochrome *c* from mitochondria. Moreover, the embryo DNA damage response influences this association after the MBT to promote cell survival (Fig. 6).

DNA damage causes cell cycle delay in G_1 before S phase, during replication, and in G_2 before mitosis. DNA damage checkpoints monitor DNA status at either G_1 or G_2 phases and prevent inappropriate transitions into S phase and mitosis when damage is detected. In addition, aberrant entry into S phase has been linked to apoptosis in many systems (8). Our results show that deregulation of the cell cycle occurs with either induction or prevention of apoptosis in embryos irradiated before or after the MBT. The fluorescence-activated cell sorter profile of isolated nuclei from irradiated embryos showed that prevention of apoptosis is linked to G_1 arrest. This result seems to be a direct consequence of the increased level of $p27^{Xic1}$ (Fig. 3) that binds to and inhibits both Cdk2 and Cdk4 (Figs. 4 and 5). These results indicate that the G_1 DNA damage checkpoint established first during *Xenopus* development monitors the G_1/S transition. We propose that, after the MBT, the biochemical events that we have shown to be triggered by γ-IR during the G_1/S transition govern the decision to commit to apoptosis.

Although $p27^{Xic1}$ is induced by DNA damage like $p21^{CIP1/WAF1}$ and has a proliferating cell nuclear antigen-binding site in its C terminus, the $p27^{Xic1}$ N-terminal Cdk-inhibitory region is most similar to Kip family members (18). The C-terminal sequence of $p27^{Xic1}$ also shares stretches of homologous sequence with Kip family members, including a conserved QTP consensus site for Cdk2 phosphorylation. $p27^{Xic1}$ degradation is cell cycle regulated, is mediated by the ubiquitin–proteasome pathway, and depends on Cdk2 activity (47), suggesting that its regulation is most like that of Kip family members. Thus the abundance of $p27^{Xic1}$ in *Xenopus* is regulated by degradation, and this mechanism may serve to control the activity of cdks during the DNA damage response. Preliminary experiments indicate that most of the increase in $p27^{Xic1}$ in response to γ-IR after the MBT still occurs in the presence of cycloheximide (data not shown). Therefore, we propose that the increase in amount of $p27^{Xic1}$ in embryos irradiated after the MBT is brought about at least in part by reduced degradation.

In conclusion, we have provided functional and biochemical evidence about the different mechanisms involved in the prevention of apoptosis in embryos irradiated after the MBT. Our data favor a model where apoptosis is prevented by the inactivation of proapoptotic components, activation of antiapoptotic elements, and regulation of cell cycle progression (Fig. 6). This concerted change in the response of the embryo to DNA damage identifies another key element in the midblastula transition in *Xenopus* development.

We thank Y.-W. Qian and E. Erikson for providing a *Xenopus* oocyte library and M. Schwab and E. Erikson for a critical reading of the manuscript. We also thank Janet Kyes for assistance with antibody purification. This work was supported by a grant from the National Institutes of Health (GM26743). C.V.F. is an Associate, and J.L.M. is an Investigator of the Howard Hughes Medical Institute.

1. Thornberry, N. A. & Lazebnik, Y. (1998) *Science* **281,** 1312–1316.
2. Zou, H., Henzel, W. J., Liu, X., Lutschg, A. & Wang, X. (1997) *Cell* **90,** 405–413.
3. Vaux, D. L., Weissman, I. L. & Kim, S. K. (1992) *Science* **258,** 1955–1957.
4. Adams, J. M. & Cory, S. (1998) *Science* **281,** 1322–1326.
5. Franke, T. F., Kaplan, D. R. & Cantley, L. C. (1997) *Cell* **88,** 435–437.
6. Marte, B. M. & Downward, J. (1997) *Trends Biochem. Sci.* **22,** 355–358.
7. Kandel, E. S. & Hay, N. (1999) *Exp. Cell Res.* **253,** 210–229.
8. Meikrantz, W. & Schlegel, R. (1995) *J. Cell Biochem.* **58,** 160–174.
9. Linette, G. P., Li, Y., Roth, K. & Korsmeyer, S. J. (1996) *Proc. Natl. Acad. Sci. USA* **93,** 9545–9552.
10. O'Reilly, L. A., Huang, D. C. & Strasser, A. (1996) *EMBO J.* **15,** 6979–6990.
11. Gil-Gomez, G., Berns, A. & Brady, H. J. (1998) *EMBO J.* **17,** 7209–7218.
12. Kuerbitz, S. J., Plunkett, B. S., Walsh, W. V. & Kastan, M. B. (1992) *Proc. Natl. Acad. Sci. USA* **89,** 7491–7495.
13. el-Deiry, W. S., Tokino, T., Velculescu, V. E., Levy, D. B., Parsons, R., Trent, J. M., Lin, D., Mercer, W. E., Kinzler, K. W. & Vogelstein, B. (1993) *Cell* **75,** 817–825.
14. Clarke, A. R., Purdie, C. A., Harrison, D. J., Morris, R. G., Bird, C. C., Hooper, M. L. & Wyllie, A. H. (1993) *Nature (London)* **362,** 849–852.
15. Lowe, S. W., Schmitt, E. M., Smith, S. W., Osborne, B. A. & Jacks, T. (1993) *Nature (London)* **362,** 847–849.
16. Tchang, F., Gusse, M., Soussi, T. & Mechali, M. (1993) *Dev. Biol.* **159,** 163–172.
17. Anderson, J. A., Lewellyn, A. L. & Maller, J. L. (1997) *Mol. Biol Cell* **8,** 1195–1206.
18. Su, J. Y., Rempel, R. E., Erikson, E. & Maller, J. L. (1995) *Proc. Natl. Acad. Sci. USA* **92,** 10187–10191.
19. Newport, J. & Kirschner, M. (1982) *Cell* **30,** 675–686.
20. Newport, J. & Kirschner, M. (1982) *Cell* **30,** 687–696.
21. Hensey, C. & Gautier, J. (1997) *Mech. Dev.* **69,** 183–195.
22. Nieuwkoop, P. D. & Faber, J. (1975) in *Normal Table of Xenopus laevis*, eds. Nieuwkoop, P. D. & Faber, J. (North-Holland, Amsterdam), pp.163–188.
23. Gautier, J., Minshull, J., Lohka, M., Glotzer, M., Hunt, T. & Maller, J. L. (1990) *Cell* **60,** 487–494.
24. Rempel, R. E., Sleight, S. B. & Maller, J. L. (1995) *J. Biol. Chem.* **270,** 6843–6855.
25. Gabrielli, B. G., Roy, L. M., Gautier, J., Philippe, M. & Maller, J. L. (1992) *J. Biol. Chem.* **267,** 1969–1975.
26. Andrews, M. T. & Brown, D. D. (1987) *Cell* **51,** 445–453.
27. Alessi, D. R., Andjelkovic, M., Caudwell, B., Cron, P., Morrice, N., Cohen, P. & Hemmings, B. A. (1996) *EMBO J.* **15,** 6541–6551.
28. Andersen, C. B., Roth, R. A. & Conti, M. (1998) *J. Biol. Chem.* **273,** 18705–18708.
29. Oltvai, Z. N., Milliman, C. L. & Korsmeyer, S. J. (1993) *Cell* **74,** 609–619.
30. Kozak, M. (1987) *Nucleic Acids Res.* **15,** 8125–8148.
31. Reed, S. I., Bailly, E., Dulic, V., Hengst, L., Resnitzky, D. & Slingerland, J. (1994) *J. Cell Sci. Suppl.* **18,** 69–73.
32. Hartley, R. S., Sible, J. C., Lewellyn, A. L. & Maller, J. L. (1997) *Dev. Biol.* **188,** 312–321.
33. Sherr, C. J. & Roberts, J. M. (1999) *Genes Dev.* **13,** 1501–1512.
34. Hartley, R. S., Rempel, R. E. & Maller, J. L. (1996) *Dev. Biol.* **173,** 408–419.
35. Pines, J. (1993) *Trends Biochem. Sci.* **18,** 195–197.
36. Ewen, M. E., Sluss, H. K., Sherr, C. J., Matsushime, H., Kato, J. & Livingston, D. M. (1993) *Cell* **73,** 487–497.
37. Grafstrom, R. H., Pan, W. & Hoess, R. H. (1999) *Carcinogenesis* **20,** 193–198.
38. Datta, S. R., Dudek, H., Tao, X., Masters, S., Fu, H., Gotoh, Y. & Greenberg, M. E. (1997) *Cell* **91,** 231–241.
39. Kennedy, S. G., Wagner, A. J., Conzen, S. D., Jordan, J., Bellacosa, A., Tsichlis, P. N. & Hay, N. (1997) *Genes Dev.* **11,** 701–713.
40. del Peso, L., Gonzalez-Garcia, M., Page, C., Herrera, R. & Nunez, G. (1997) *Science* **278,** 687–689.
41. Kennedy, S. G., Kandel, E. S., Cross, T. K. & Hay, N. (1999) *Mol. Cell. Biol.* **19,** 5800–5810.
42. Fujita, E., Jinbo, A., Matuzaki, H., Konishi, H., Kikkawa, U. & Momoi, T. (1999) *Biochem. Biophys. Res. Commun.* **264,** 550–555.
43. Alessi, D. R., Caudwell, F. B., Andjelkovic, M., Hemmings, B. A. & Cohen, P. (1996) *FEBS Lett.* **399,** 333–338.
44. Nakajima, K., Takahashi, A. & Yaoita, Y. (2000) *J. Biol. Chem.* **275,** 10484–10491.
45. Cardone, M. H., Roy, N., Stennicke, H. R., Salvesen, G. S., Franke, T. F., Stanbridge, E., Frisch, S. & Reed, J. C. (1998) *Science* **282,** 1318–1321.
46. Sible, J. C., Anderson, J. A., Lewellyn, A. L. & Maller, J. L. (1997) *Dev. Biol.* **189,** 335–346.
47. Yew, P. R. & Kirschner, M. W. (1997) *Science* **277,** 1672–1676.